

01,07

## Non-adiabatic dynamics of atoms and phase transformations kinetics in solids

© Yu.A. Khon

Institute of Strength Physics and Materials Science, Siberian Branch, Russian Academy of Sciences, Tomsk, Russia

E-mail: khon@ispms.ru

Received January 26, 2024

Revised January 26, 2024

Accepted January 27, 2024

A model of phase transformations in solids is proposed, taking into account the relationship of non-linear processes that occur on various spatio-temporal scales in the non-linear open system of nuclei and electrons. The characteristic times of structural changes are determined by two mechanisms of atoms displacements: thermally activated in thermal fluctuations and athermic during non-adiabatic Landau–Zener transitions of atoms. Cooperative processes on a large spatio-temporal scale are described by two order parameters. The macroscopic kinetics of phase transformation is determined by two coupled nonlinear equations of the parabolic type for order parameters. These equations have two types of solutions describing the characteristic features of morphological changes in a solid with diffusion and martensitic phase transformations. The origin and growth of the new phase during diffusion phase transformations are described by solutions in the form of a switching wave from the metastable phase to a stable one. The formation of the embryo of the new phase is determined by structural changes on the atomic scale. Thermoelastic and reconstructive martensitic transformations are described by solutions in the form of static autosolitons — localized distributions of order parameters. Thermoelastic martensitic transformations develop against the background of a changing short-range order, determined by athermic displacements of atoms. Reconstructive martensitic transformations are determined by athermic displacements in the unstable phase, and the presence of any sources of initial disturbances is not required.

**Keywords:** Phase transformations, non-adiabatic dynamics of atoms, athermic displacements, order parameters, kinetics, diffusion transformations, thermoelastic martensitic transformations, reconstructive martensitic transformations.

DOI: 10.61011/PSS.2024.03.57933.7

### 1. Introduction

The first-order phase transitions (PT) in solids (polymorphous, diffusion and martensitic transformations, crystallization of the amorphous phase, decomposition of the solid solution, etc.) are very common in nature and play a key role in changing the microstructure and properties of various materials. Therefore, a lot of attention was and is paid to experimental and theoretical study of the phase transformations [1–18]. It is established that depending on a chemical composition, temperature and velocity of heating/cooling, the mechanisms and kinetics of the phase transformation can be various, thereby affecting a morphology of the obtained product. At comparatively high temperatures and in conditions close to the equilibrium ones (the low velocities of heating/cooling), the phase transformation belongs to the diffusion ones, whose mechanism is considered to be thermally activated displacements of atoms. Within the temperature range  $\Delta T$ , the new phase grows by means of the old phase. The metastable phase becomes unstable in relation to small perturbations of the density outside the range  $\Delta T$  at the temperatures below (above)  $T_{in}$  during cooling (heating). The phase transformations determined by athermic shift displacements of the atoms belong to

the martensitic (diffusionless) ones. The distinctive feature thereof is that within the range of transformation, from the very beginning, crystals of the new phase are formed and they do not grow with further change of the temperature. A portion of the new phase is increased by means of formation of new crystals. The deformation of the crystals is predominantly of a shift nature and volume changes of the phase transformation are low. There are thermoelastic and reconstructive martensitic transformations. The systems with the thermoelastic martensite transformation (TMT) are typically represented by titanium-based alloys. The TMTs can develop in the conditions which are close to the equilibrium ones. The equilibrium diagram of alloy state has a two-phase area separating the austenite phase from the martensite phase. At  $T < A_f$  ( $T > M_f$ ), there is only one martensite (austenite) phase. Within the range  $M_s < T < A_s$ , the austenite and martensite phase are in equilibrium. Here,  $A_s, A_f$  ( $M_s, M_f$ ) are commonly accepted as designations for the temperatures of the start and end of the range of transformation of austenite (martensite) into martensite (austenite), respectively. The transition from the austenite (martensite) phase into the martensite (austenite) phase is preceded with a pre-transition state. This state exhibits a short-range order, which is non-typical

for the austenite (martensite) phase. In the reconstructive martensitic transformations (RMT), the phase with another crystal structure (FCC  $\rightarrow$  BCC, BCC  $\rightarrow$  HCP and so on) is formed in fast cooling to the low temperatures. For example, the ferrum alloys exhibit embeddings, substitutions of RMTs during cooling to the temperatures within the range  $M_s - M_f$ . The temperature difference can be up to hundreds of Kelvins. When cooling below the temperature  $M_f$ , the new phase is not formed. In RMT, the volumetric portion of the martensite phase is always less than one. The equilibrium diagrams of the state has no two-phase area. Neither a pre-transition state, nor an embryo of the new phase is observed. In some solids, depending on the temperature and velocity of cooling, the phase transformations can proceed both in one and another mechanism.

The existing variety of the phase transformations is due to a plurality of complex interrelated non-linear processes that occur on various spatio-temporal scales. In the end, the macroscopic kinetics of the phase transformation is determined by the dynamics of atoms. Most existing models of the phase transformations assume that the dynamics of atoms and, consequently, the kinetics of transformation is determined only by vibrational degrees of freedom, and contribution of the electron degrees of freedom to the dynamics of atoms is not taken into account and it is implicitly assumed that adiabatic approximation is feasible (electrons instantly adjust to slow movement of nuclei). In this case, the transition from the metastable phase into the stable one is possible in the mechanism of heterogeneous nucleation. The new phase starts growing, if the embryo of the new phase formed in the metastable phase by means of thermal fluctuations exceeds a critical value. Defects of various types present in the metastable phase can lower a height of the potential barrier, increasing the probability of critical nucleation. The transitions through the potential barriers of the intermediate states also increase the probability of nucleation [12–15]. The defects and the intermediate states are also responsible for increased velocities of movement of interphase boundaries, which are observed in some cases. At the same time, applicability of the model of heterogeneous nucleation to the martensitic transformations is doubtful. In particular, at the low temperatures and the high velocities of cooling the velocity of critical nucleation can be much less than the observed velocity of transformation, which is comparable to the speed of sound in many cases.

In the phase transformation, the solid is an open system of nuclei and electrons. This system has two ways of displacement of atoms out of equilibrium positions. As in the isolated system, the first way is determined by thermal fluctuations in vibrations of atoms. It implements the thermally activated mechanism of atoms displacements. The probability of the displacements decreases exponentially with reduction of the temperature. The second way is determined by nonadiabatic Landau–Zener (LZ) transitions of atoms in electronic transitions between intersecting surfaces

of potential energy [19–24]. At that, the potential energy of the system always decreases. It implements the athermal mechanism of atoms displacements. The probability of the nonadiabatic LZ transitions does not depend on the temperature. The change of interatomic interactions in the nonadiabatic LZ transitions results in displacements of the nuclei, removes the system from a previous equilibrium state and it is accompanied by reduction of the potential energy of the system. For brevity, the atoms displacements in the nonadiabatic LZ transitions [25,26] have been called dynamic displacements (DD). In the open system, the change of the crystal structure (phase transformation) is possible without critical nucleation. Let us note that the Zeldovich theory [1] does not exclude such an option of the phase transformation. The theory assumes that the system has a subcritical embryo. The mechanism of its nucleation can be both the thermally activated and athermal one. The kinetics of the embryo growth is determined by the velocity of transition of atoms from the metastable phase to the embryo, while the velocity itself depends on the mechanisms of embryo growth. There were no restrictions of the mechanisms of embryo growth and its sizes. The very mechanisms are determined by the dynamics of the atoms.

The paper [26] has suggested the mechanism of nucleation of the new phase in the solid, which is determined by the nonadiabatic Landau–Zener transitions in the open system of nuclei and electrons. It has found conditions for nucleation of stable and unstable embryos. The present paper continues [26] and it aims at solving a problem of the kinetics of the phase transformation in the thermally activated and athermal displacements of the atoms.

## 2. Model of phase transformation

It considers a homogeneous solid, in which only the topological short-range order changes at PT. The solid can be either single-component or multicomponent, both crystalline and amorphous. The phase transformations proceeding within the temperature range  $\Delta T$  are accompanied by the change of the volume  $\Delta V$ , absorption/release of heat. There are simultaneously the new and old phases within the range  $\Delta T$ . The curve of the dependence of  $V$  on  $T$  has a hysteresis loop. It is assumed that macroscopic characteristics of the system  $\Delta T, \Delta V$  are known. The two phases are in equilibrium at the temperature  $T_0$ . The phase of nucleation of the new phase will be called a parent one. Then, in cooling the phase stable at  $T > T_0$  will be a parent one, so in heating will it — at  $T < T_0$ . Let us introduce a dimensionless temperature  $\theta = \frac{T-T_0}{T_0}$ , ( $\theta = \frac{T_0-T}{T_0}$ ) and the rate of its change  $\dot{\theta} = \dot{T}/T_0$  ( $\dot{T} = dT/dt$ ,  $t$  — time) during heating (cooling) of the system. In the phase transformation, the volume of the system  $V(\theta)$  changes from  $V_p(\theta)$  in the parent phase to  $V_n(\theta)$  in the new phase. It is assumed that the equations of the state  $V_p = V_p(\theta)$ ,  $V_n = V_n(\theta)$  are known. The relative change

of the volume  $\vartheta(\theta) = [V(\theta) - V_p(\theta)]/V_p(\theta)$  characterizes a system response to processes that occur in the medium at the temperature  $\theta$ .

The relative change of the volume  $\vartheta_n = [V_n - V_p]/V_p$  in the phase transformation is determined by a sum of diagonal elements of a tensor of macroscopic deformation by the phase transformation. The paper [27] deals with three main values of the deformation tensor  $\varepsilon_j$  in the coordinate system related to the main axes. Here  $j = 1, 2, 3$ . The local change of the volume of the system  $\vartheta(\mathbf{r}, \theta)$  is equal to the first invariant of the deformation tensor  $I_1(\mathbf{r}, \theta) = \varepsilon_1(\mathbf{r}, \theta) + \varepsilon_2(\mathbf{r}, \theta) + \varepsilon_3(\mathbf{r}, \theta)$ , while the local shear strain is determined by the second invariant  $I_2(\mathbf{r}, \theta) = \varepsilon_1(\mathbf{r}, \theta)\varepsilon_2(\mathbf{r}, \theta) + \varepsilon_1(\mathbf{r}, \theta)\varepsilon_3(\mathbf{r}, \theta) + \varepsilon_2(\mathbf{r}, \theta)\varepsilon_3(\mathbf{r}, \theta)$ . Here,  $\mathbf{r}$  is a radius-vector in the Cartesian coordinate system  $x = x_1, y = x_2, z = x_3$ . The functions  $I_1(\mathbf{r}, \theta), I_2(\mathbf{r}, \theta)$  specify spatial distribution of the new phase, so do  $\langle I_1(\mathbf{r}, \theta) \rangle, \langle I_2(\mathbf{r}, \theta) \rangle$  — a volume portion of the new phase. The character  $\langle \dots \rangle$  designates averaging across the system volume. In this case,  $\vartheta = \langle I_1(\mathbf{r}, \theta) \rangle$ . A rate of processes that occur in the phase transformation should satisfy the inequality  $\langle \dot{I}_1(\mathbf{r}, t) \rangle \geq \dot{V}_p$ . The magnitude  $\dot{V}_p = dV_p/dt$  is specified by the velocity of heating/cooling of the system.

The deformation by the phase transformation is determined by displacements of the atoms out of the positions  $\mathbf{R}_0 = \{\mathbf{R}_{01}, \dots, \mathbf{R}_{0N}\}$  into the positions  $\mathbf{R}_n = \{\mathbf{R}_{n1}, \dots, \mathbf{R}_{nN}\}$  in the new phase. The atoms paths pass from the potential energy surface (PES) of the parent phase  $E_0(\mathbf{R})$  to PES of the new phase  $E_n(\mathbf{R})$ . Each PES is a surface in the  $3N$  — dimensional space with one's minimums and potential barriers separating them [28,29]. The potential energy of the parent (new) phase in the minimum point  $\mathbf{R} = \mathbf{R}_0$  ( $\mathbf{R} = \mathbf{R}_n$ ) is equal  $E_0[\mathbf{R}_0]$  ( $E_n[\mathbf{R}_n]$ ). In the open system of nuclei and electrons, the paths of all the atoms must pass through the PESes  $E_\gamma(\mathbf{R}_\gamma)$  between the PESes  $E_0$  and  $E_n$ . Here,  $\gamma = 1, \dots, m-1$  is a PES number. For the PES  $E_0(E_n)$   $\gamma = 0(m)$ . The PESes differ by distribution of the nuclei, the electrons and the interatomic interactions. An average value of the energy range between the two adjacent PESes  $\Delta E_\gamma \approx (E_n - E_0)/N$ . The height of the potential barrier separating the minimums at the two adjacent PESes is  $\Delta E_\gamma$  in terms of the magnitude order. With the big number of the PESes,  $\Delta E_\gamma \ll k_B T$ ,  $k_B$  is the Boltzmann constant. When the system volume changes, as a result of heating/cooling the PESes are displaced in relation to each other and intersect. In these conditions, there are two possible mechanisms of transitions from one PES to another.

The thermally activated mechanism of the displacements is determined by the transitions of the atoms between the PESes in thermal fluctuations. At the same time, the electron subsystem instantly adjusts to another distribution of the nuclei. The probability  $P_{1th}$  and the time of the transition  $t_{1th}$  between the adjacent PESes are determined

by the known expressions

$$P_{1th} \propto \exp\left(-\frac{\Delta E_\gamma}{k_B T}\right), \quad (1)$$

$$t_{1th} \propto \exp\left(\frac{\Delta E_\gamma}{k_B T}\right). \quad (2)$$

The athermic mechanism of the displacements is determined by the probability  $P$  of the nonadiabatic transition of the atoms between the two intersecting PESes due to the electron subsystem with subsequent nuclei displacement. For the system of two atoms whose energy levels near the intersection point have the same signs of derivatives of potential energy along the coordinate [19]:

$$P = \exp(-2\pi W_0^2 / (\hbar v |F_2 - F_1|)). \quad (3)$$

Here  $v$  — the displacement velocity of atoms determined by the rate of volume change during heating/cooling,  $F_1, F_2$  — the derivatives of potential energy along the coordinate near the intersection point of the energy levels 1 and 2, respectively,  $2W_0$  — the width of the energy gap between the levels. The characteristic time of a single transition

$$t_{1LZ} = W_0 / (v |F_2 - F_1|) \quad (4)$$

does not depend on the temperature and decreases with increase in  $v$ . In two independent processes

$$1/t_1 = 1/t_{1LZ} + 1/t_{1th}. \quad (5)$$

It is clear from (2)–(5) that at the high temperatures and the low velocities of heating/cooling  $t_{1th} \ll t_{1LZ}$  and  $t_1 = t_{1th}$ . At the low temperatures and/or the high velocities of heating/cooling  $t_1 = t_{1LZ}$ . The nonadiabatic transitions of atoms determine the athermic mechanism of displacements, which is inherent in the martensitic transformations.

Taking into account the above said, the displacements of atoms  $\mathbf{u}(t) = \mathbf{R}_n(t) - \mathbf{R}_0(t)$  are written as

$$\mathbf{u}(t) = \mathbf{u}_d(t) + \mathbf{u}_{el}(t). \quad (6)$$

Here,  $\mathbf{u}_d = \{\mathbf{u}_{d1}, \dots, \mathbf{u}_{dn}\}$  — the dynamic displacements of atoms due to the change of the interatomic interactions,  $\mathbf{u}_{el}$  — the displacements determined by the vibrational degrees of freedom. The distribution of atoms with the coordinates  $\mathbf{R}_0 + \mathbf{u}_d$  determines a dynamic short-range order (DSO), which is non-typical for the parent phase [25]. At the threshold values  $\mathbf{u}_d$ , the DSO system becomes unstable in relation to the small displacements in vibrations of atoms. The DD is to be found by reducing to solving equations of the nonadiabatic dynamics of atoms (NDA), which have the system volume as a governing parameter. But, due to nonlinearity of the NDA equations, any small perturbations (for example, replacement of the PES set) result in different large-scale DD distributions. As a result, the dynamics of the system is ambiguously predicted on large spatial and/or time scales. In this situation, in order to

find the large-scale DD distributions, which determine the macroscopic properties of the system, it uses an approach developed in the theory of nonlinear systems [30]. For clarity of further discussion, we note main points. As in [26], the one-dimensional case is considered.

## 2.1. Order parameters

Let us designate the homogeneous stationary DD distributions at  $\theta > 0$  as  $\bar{u}_d$ . Let us consider a static wave of the displacements  $\delta u(x) \propto \exp(ikx)$  with the wavelength  $\lambda \propto 1/k > l_0$ . Here,  $l_0$  — the interatomic distance. At  $\theta < \theta_1$  any perturbation  $\delta u$  results in increase in the system's potential energy, whereas the metastable phase is stable in relation to the small perturbations. At the stability threshold  $\theta_1$ , the distribution of the atoms, which is typical for the parent phase, is unstable in relation to the small perturbations  $\propto \exp(k_1x)$  with the wave vector  $k_1$ . At  $\theta > \theta_1$ , the system's potential energy is reduced, and the metastable phase is unstable in relation to the small perturbations. Near the dimensionless threshold of stability  $a_1 = \frac{\theta - \theta_1}{\theta_1} \ll 1$ , the perturbations of the frequency  $\omega_1 \propto 1/t_1$  increase. The resultant perturbation of the distribution is found as superposition of plane waves with the wave vectors  $k = k_1 \pm \Delta k$  ( $\frac{\Delta k}{k_1} \ll 1$ ). As known, this superposition describes beatings with the amplitude  $\varphi(x, t)$ . The amplitude of the unstable mode  $\varphi(x, t)$  characterizes correlated (collective) distributions of atoms in the parent phase on the spatial scales  $l_1 \propto \frac{1}{k_1} > l_0$ . Near the dimensionless threshold of stability, the large-scale spatial distribution of the displacements  $u_d(x, t)$  can be written as in [30]:

$$u_d(x, t) - \bar{u}_d = u_d^0 [\varphi(x, t) \exp(ik_1x) + cc], \quad (7)$$

where  $u_d^0$  — the parameter determined by the medium properties,  $cc$  signifies complex conjugate. In the stable parent phase,  $\varphi = 0$ . Note that in addition to the distribution (7), other distributions are also possible. But, the frequency  $\omega_1$  is the highest of all possible. That is why the time of formation of the distribution (7) is the least. For this reason, it is this time that exhibits in the experiment. All other distributions either fail to exhibit, or the distribution thereof is low.

The localized displacements of atoms (7) result in long-range stresses and heterogeneous deformation  $\varepsilon_j(\mathbf{r}, \theta)$ . The solution of the equations of the continuum mechanics can be avoided by considering the collective modes of deformation, which are determined by the vibrational degrees of freedom. Let us designate the main values of the tensor of homogeneous deformation as  $\bar{\varepsilon}_1, \bar{\varepsilon}_2, \varepsilon_3$ . At  $\vartheta < \vartheta_c$ , the medium deformation is still homogeneous, while the small perturbation  $\propto \exp(ikx)$  with any wave vector  $k$  results in increase in the system's potential energy. The threshold of stability  $\vartheta_c$  has an unstable mode of displacements  $\propto \exp(ik_2x)$  with the wave vector  $k_2 < k_1$ . At  $\vartheta > \vartheta_c$ , the small perturbations of the frequency  $\omega_2 \propto 1/t_2$  increase. Near the dimensionless threshold of stability  $a_2 = \frac{\vartheta(\varphi) - \vartheta_c}{\vartheta_c} \ll 1$ ,

the deformation is determined by superposition of the plane waves with the wave vectors  $k = k_2 \pm \Delta k$  ( $\frac{\Delta k}{k_2} \ll 1$ ). The spatio-temporal distribution of the main deformations in the phase transformation is written as

$$\varepsilon_j(x, t) - \bar{\varepsilon}_j = \varepsilon_j^0 [\eta(x, t) \exp(ik_2x) + cc]. \quad (8)$$

Here, the coefficient  $\varepsilon_j^0$  determines the value of the main deformations,  $\eta(x, t)$  — the amplitude of the unstable mode, which characterizes heterogeneous deformation of the medium on the spatial scales  $l_2 \propto \frac{1}{k_2} > l_1$ . The first and the second invariants of deformation  $I_1(x, t), I_2(x, t)$  are found in a standard way. As per Landau, in the physics the amplitudes of the unstable modes are commonly referred to as order parameters (OP). In the linear approximation, the dimensionless threshold of stability  $a_2$  can be written as

$$a_2 = -1 + \frac{\vartheta(\varphi)}{\vartheta_c} = -1 + p\varphi, \quad p = \frac{1}{\vartheta_c} \frac{d\vartheta(\varphi)}{d\varphi}. \quad (9)$$

It follows from the definition of  $a_2$  that the magnitude  $p > 0$ , and the sign of the derivative  $\frac{d\vartheta(\varphi)}{d\varphi}$  must coincide with the sign of  $\vartheta_c$ .

## 2.2. Equations for the order parameters

When finding the OP equations, we assume that the open system has processes, in which the potential energy of the system of atoms is reduced. Usually, the relative change of the volume and the value of the shear strain at PT does not exceed ten percent. It can be assumed that the OPs  $\varphi, \eta$  are small parameters. So, in order to find the OP equations, it is allowed to use the Ginzburg–Landau approach and the Landau–Khalatnikov approach. Taking into account (9), the OP equations obtained in this way are as follows [26]:

$$t_1 \partial_t \varphi = [\alpha - g\eta]\varphi + q_2 \varphi^2 - q_3 \varphi^3 + l_1^2 \partial_x^2 \eta, \quad (10)$$

$$t_2 \partial_t \eta = (-1 + p\varphi)\eta - b\eta^3 + l_2^2 \partial_x^2 \eta. \quad (11)$$

The typical velocity  $v_2 = l_2/t_2$  of the equation (11) is a group velocity. In the dimensionless variables,

$$\tilde{t} = t/t_2, \quad \tilde{x} = x/l_2, \quad \tilde{\eta} = \eta b^{1/2}, \quad \tilde{\varphi} = \varphi q_3^{1/2} \quad (12)$$

the equations (10) and (11) are transformed as follows (the sign „ $\sim$ “ is omitted hereinafter)

$$\tau \partial_t \varphi = (\alpha - c\eta)\varphi + \beta \varphi^2 - \varphi^3 + l^2 \partial_x^2 \eta, \quad (13)$$

$$\partial_t \eta = (-1 + d\varphi)\eta - \eta^3 + \partial_x^2 \eta. \quad (14)$$

Here

$$\tau = \frac{t_1}{t_2}, \quad l = \frac{l_1}{l_2}, \quad \beta = q_2 q_3^{-1/2}, \quad d = p q_3^{-1/2}, \quad c = g b^{-1/2}. \quad (15)$$

The coefficients of the equations (13), (14) are parameters, which are determined by the properties of the parent and

the new phase. It is assumed that these parameters are either known, or they can be calculated. The parameter  $c \propto \vartheta_n$  of (13) characterizes increase in the system's elastic energy in nucleation of the new phase. The meaning of the parameters  $\alpha, \beta$  is considered below. The equation (13) describes the dynamics of a bistable medium. The bistability is determined by the fact that in the phase transition the paths of the atoms can simultaneously stay on the PESes  $E_0(\mathbf{R}_0)$  and  $E_\gamma(\mathbf{R}_\gamma)$  with  $\gamma > 0$ . The equation (14) represents the real Ginzburg–Landau equation [30].

### 3. Homogeneous stationary solutions

The equation (13) at  $c = 0$  has three homogeneous stationary solutions:  $\varphi_0 = 0$ ,

$$\varphi_h = \frac{\beta}{2} + \left(\frac{\beta^2}{4} + \alpha\right)^{1/2}, \quad \varphi_{in} = \frac{\beta}{2} - \left(\frac{\beta^2}{4} + \alpha\right)^{1/2},$$

as shown on Figure 1. The parameter  $\beta$  determines a numerical value of  $\varphi$ . Stability of the solutions is analyzed to show the following. The solution  $\varphi_{in}$  (a dashed curve 3 of Figure 1) is always unstable. The solution  $\varphi_0$  is the only one and stable at  $\alpha < \alpha_1 = -\frac{\beta^2}{4}$  (the area I of Figure 1), which takes place for the stable parent phase at  $\theta < \theta_0$ . At  $\alpha_1 < \alpha < 0$ , the medium is in the bistable state (the areas II, III of Figure 1). If  $\alpha_1 < \alpha < \alpha_2 = -\frac{2\beta^2}{9}$ , then the solution  $\varphi_0$  is stable, and  $\varphi_h$  is metastable (the curve 1 of Figure 1). At  $\alpha_2 < \alpha < 0$ , the solution  $\varphi_h$  is stable (the curve 2 of Figure 1),  $\varphi_0$  — metastable. At  $\alpha = \alpha_2$ , both the solutions have the same stability. At  $\alpha > 0$ , (the area IV of Figure 1) the solution  $\varphi_h(\varphi_0)$  is stable (unstable), and any small perturbation  $\alpha$  increases. Therefore, the parameter  $\alpha = \alpha(\theta)$ . The temperature  $\theta_0$  is found from the equality  $\alpha = -2\beta^2/9$ . The equation  $\alpha(\theta) = 0$  is used to find the temperature  $\theta_{in}$  of stability loss of the parent phase in relation to the small perturbations. The sign „–“ in front of the coefficient  $c$  in the right side of the equation (13) shows that the elastic deformation of the medium increases the potential energy ( $\propto -\int \partial_t \varphi d\varphi$ ) of the system.

The equation (14) at  $d = 0$  has the only stable solution  $\eta_0 = \eta = 0$ . At  $d > 1/\varphi$ , there is a solution  $\eta > 0$ , which is matched with a smaller value of the potential energy ( $\propto -\int \partial_t \eta d\eta$ ). The magnitude  $d\varphi - 1 > 0$  determines the rate of OP increase  $\eta$ .

The equations (13), (14) always have the homogeneous stationary solution (HSS)  $\eta_0, \varphi_0$ , which corresponds to the parent phase. The stability has been analyzed in a standard way to show that the solution  $\eta_0, \varphi_0$  is stable in relation to the small homogeneous and heterogeneous perturbations of the frequency  $\omega$  and with the wave vector  $k$  at

$$-\tau + \alpha < 0, \tag{16}$$

$$-\alpha > 0. \tag{17}$$

At  $\alpha < 0$ , these inequalities are always satisfied, which takes place for the parent phase in the stable and the metastable

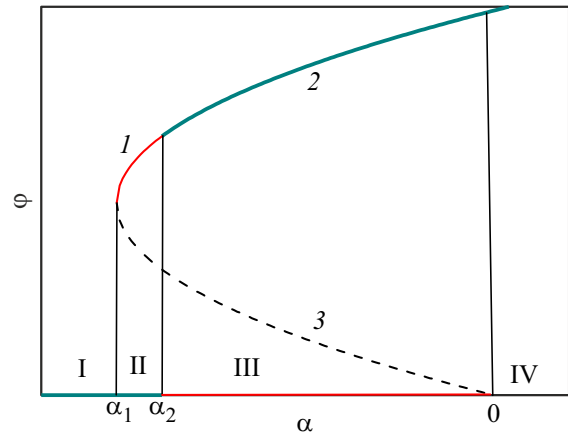


Figure 1. Dependence of the order parameter  $\varphi$  on  $\alpha$ . See the article text for explanations.

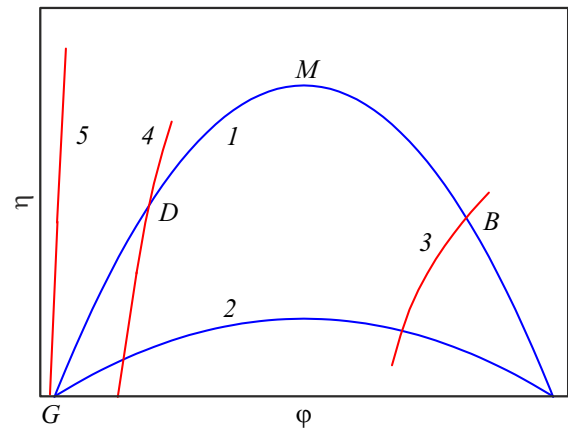


Figure 2. Zero-isoclines of the equations (17) — the blue curves (1, 2) and (18) — the red curves (3, 4, 5).

state. Other HSSes are determined by points of curve intersection (zero-isocline):

$$(\alpha - c\eta)\varphi + \beta\varphi^2 - \varphi^3 = 0, \tag{18}$$

$$(-1 + d\varphi)\eta - \eta^3 = 0. \tag{19}$$

The plot curves (18), (19) at  $\alpha < 0$  and characteristic points of intersection are shown on Figure 2. The parabola (18) intersects the straight line  $\eta = 0$  in the points  $\varphi = \varphi_{in}$  and  $\varphi = \varphi_h$ . The curve (19) at

$$d_G > d_D > d_B > d_0 \tag{20}$$

and fixed values of the other three parameters can intersect the parabola (18) in the three characteristic points B, D, G. Here,  $d_0$  — the value of  $d$ , below which the curves (18), (19) do not intersect. When

$$d = d_m = \frac{2}{\beta} \left[ 1 + \left( \frac{\beta^2 - 4\alpha}{4c} \right)^2 \right] \tag{21}$$

the curves intersect at the vertex of the parabola (the point M) at  $\varphi = \beta/2$ . Taking into account (8), the smaller value of  $\vartheta_c$  is matched with the bigger value of  $d$ .

HSS stability is analyzed to show the following. The solution  $\eta_B > 0$ ,  $\varphi_B > 0$  in the point B is stable in relation to the small homogeneous and heterogeneous perturbations. The HSS  $\eta_D > 0$ ,  $\varphi_D > \varphi_{in}$  in the point D is stable in relation to the small homogeneous perturbations, but it is unstable in relation to the heterogeneous perturbations. In this case,  $\varphi_D < \varphi_B$ . The point G (HSS  $\eta_G = 0$ ,  $\varphi_G < \varphi_{in}$ ) has no stable solution [26,31]. This situation is possible in the systems without the phase transformations, for example, when the high-temperature phase is quenched.

#### 4. Heterogeneous solutions

The heterogeneous solutions  $\varphi(x, t)$ ,  $\eta(x, t)$  describe the transitions of the system from the metastable state  $\eta_0, \varphi_0$  into the states in the points B and D. The transition into the point B includes formation and propagation of a switching wave (SW)  $\varphi(x - v_{sw}t)$ ,  $\eta(x - v_{sw}t)$ , whose velocity is  $v_{sw}$ . In front of (behind) the front, the medium is in the state  $\eta_0, \varphi_0$  ( $\varphi_B > 0$ ,  $\varphi_D > 0$ ). The OPs change at the SW front. The transition into the point D can include excitation of localized solutions  $\varphi(x, t)$ ,  $\eta(x, t)$  — autosolitons (AS) [32]. They are non-equilibrium localized states of a nonlinear medium. SW and AS nucleation requires initial OP perturbation  $\varphi$  with the amplitude

$$\Delta\varphi_0 > \varphi_{in}. \quad (22)$$

For this,  $N_{in}$  of the atoms should be displaced into positions, which are non-typical for the parent phase. The probability of the displacement of  $N_{in}$  of the atoms is determined by a product of the probabilities (1) or (3). Then, in the nonadiabatic transitions of the atoms the time of origin of the initial perturbation (22):

$$t_{LZ} = N_{in}W_0/(v|F_2 - F_1|), \quad (23)$$

and in the thermally activated displacements

$$t_{th} \propto \exp\left(\frac{N_{in}\Delta E_\gamma}{k_B T}\right). \quad (24)$$

The product  $N_{in}\Delta E_\gamma$  means energy of critical nucleation. It follows from the formulas (23), (24) that at  $N_{in} \gg 1$  the time of origin of the initial perturbation (22) in thermal fluctuations will be great in comparison with (23). So, the condition (22) is fulfilled by the time (23). This conclusion should not be surprising, as the parent and the new phases differ by the interatomic interactions.

#### 5. Diffusion phase transformations

The diffusion phase transformations occur at comparatively high temperatures, low rates of temperature change

and are characterized by a wide loop of hysteresis and larger volume changes in comparison with the martensitic transformations. In these conditions, taking into account (8), the coefficient  $d$  must be small, and the transition from the metastable state comes into the point B. It is generally assumed that nucleation and growth of the new phase are determined by thermally activated processes. Indeed, in these conditions, as it follows from (4), at low velocities  $v$  of (23),  $N_{in} \approx 1$  and the inequality  $t_1 = t_{1th}$  is fulfilled. The atoms displacements are determined by the vibration degrees of freedom. The same degrees of freedom determine medium deformation. It means that the parameters  $\tau < 1$ ,  $l < 1$  must have close values, i.e.

$$\tau \lesssim l. \quad (25)$$

If this condition is fulfilled, then  $v_1 = l_1/t_1 \lesssim v_2 = l_2/t_2$ . The diffusion transformation occurs at an interface of the new phase and the matrix. When the said interface moves, the volume portion of the new (parent) phase increases (decreases). This situation of transformation is described by heterogeneous solutions in the form of the switching wave.

The dynamics of nucleation and propagation of the SW has been considered based on the numerical solution of the equations (13), (14), wherein all the parameters are determined by properties of the phases. The form of the initial perturbations is shown in Appendix. Figure 3 exemplifies the calculation results at

$$\alpha = -0.02, \quad \beta = 0.6,$$

$$c = 0.1, \quad d = 3, \quad l = 0.15, \quad \tau = 0.1. \quad (26)$$

At these parameters,  $\varphi_h \approx 0.56$ ,  $\varphi_{in} \approx 0.04$ ,  $\eta_B \approx 0.53$ ,  $\varphi_B \approx 0.43$ . The parameters of the initial perturbation  $\Delta\varphi_0 = 0.1$ ,  $\sigma_\varphi = 3$ ,  $x_0 = 50$ . It is clear from the data of Figure 3 that there are two stages of nucleation and growth of the new phase. The first stage includes, first of all, increase in OP  $\varphi$ , OP  $\eta \approx 0$  (Figure 3, left panel). When the inequality  $d\varphi > 1$  is fulfilled, OP  $\eta$  starts increasing. Its growth rate is determined by the magnitude  $(-1 + d\varphi)$ . It can be seen from the equation (14), wherein  $\dot{\eta} \sim (-1 + d\varphi)\eta$ . At the same time, OP  $\varphi$  has almost no change. By the point of time  $t = t_{inc}$ , both the OPs accept stationary values  $\eta_B, \varphi_B$ . The localized OP distribution can be considered as a formed embryo of the new phase. Note that its formation results from evolution of the non-equilibrium system on the atomic scales. It is not necessary to include representations of any sources in the form of defects. The second stage (at  $t > t_{inc}$ ) includes embryo growth due to SW propagation. The volume occupied by the new (parent) phase is increased (decreased) (Figure 3, right panel). In case of fulfillment of the condition (25), the width of the transition area between the parent and the new phase is still constant. At  $t \gg t_{inc}$  the entire volume is filled with the new phase. The time  $t_{inc}$  means an incubation period, wherein the embryo of the new phase is formed at the first stage.

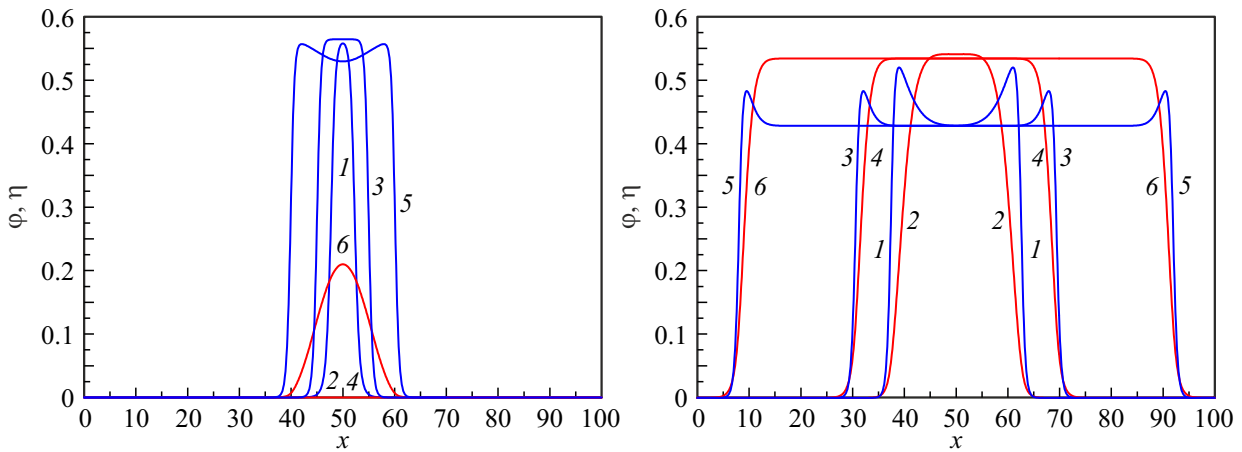


**Figure 3.** Spatial distribution of the order parameters  $\varphi$  — the blue curves (1, 3, 5),  $\eta$  — the red curves (2, 4, 6) in the switching wave in various points of time  $t$ . On the left panel,  $t = 5$  (1, 2), 10 (3, 4), 20 (5, 6). On the right panel,  $t = 25$  (1, 2), 40 (3, 4), 90 (5, 6).

If the volume is largely changed, the parameter  $d < d_0$ . In this case, there is only HSS  $\eta = 0$ ,  $\varphi = \varphi_h$ , which is stable in relation to the small perturbations. The system transition from the state  $\eta_0, \varphi_0$  into the metastable state  $\eta = 0, \varphi = \varphi_h$  occurs by nucleation and propagation of the SW  $\varphi(x - v_1 t)$ ,  $\eta = 0$ . The homogeneous solution  $\eta = 0, \varphi = \varphi_h$ , which is stable in relation to the small perturbations, can be unstable in relation to the perturbations of the OP  $\eta$  of the amplitude  $\Delta\eta > (d_B - d_0)\varphi_h$ . This perturbation can be created by excitation of a longitudinal wave due to external impact. Then, with the perturbation available, the SW is nucleated to propagate from the state  $\eta = 0, \varphi = \varphi_h$  into the state  $\eta_B, \varphi_B$ . If the perturbations are across the entire volume of the sample, the phase transformation can occur simultaneously across the entire volume. In this case, the rate of the phase transformation can be high. It is possible that such a mode of the phase transformation is observed at „explosive“ crystallization of amorphous materials [32].

When there is no source of elastic deformations (the system is homogeneous) and slow change of the temperature ( $t_{LZ} \gg t_{th}$ ), the condition (22) is not fulfilled. When  $\theta < \theta_{in}$  ( $\alpha < 0$ ), the system is still in the metastable state. When  $\theta > \theta_{in}$  ( $\alpha > 0$ ), the metastable phase is unstable in relation to the small perturbations. Any small perturbation results in the phase transformation. The diffusion transformation occurs in a mode of overcooling/overheating.

### 6. Martensitic transformations

As said above, the athermal mechanism of the martensitic transformations is determined by nonadiabatic transitions of the atoms. The shear mechanism of deformation in the martensitic transformations is explained as follows. For the systems with the martensitic transformations, the relative changes of the volume  $\vartheta_c$  of (9) usually do not exceed several percent and they are smaller than those in the diffusion ones. So, the parameter  $d \propto 1/\vartheta_c$  must be greater

than for the diffusion transformations. The interest is paid to the solutions, which describe the transition from the metastable parent phase into the point D of Figure 2. This case may include excitation of the localized solutions  $\varphi(x, t), \eta(x, t)$  — the autosolitons (AS) [33]. The kinetic variables change sharply inside the autosoliton, whereas they are equal to stationary values on its periphery (in this case they are zero). The static autosolitons describe the localized distributions of the new phase, which are typical for the martensitic transformations. The static autosolitons can be excited in case of available perturbation of the final amplitude (22), and fulfillment of the inequalities [33]:

$$\tau < 1, \quad l \ll 1, \quad \tau > l \tag{27}$$

and the condition

$$d > 1/\varphi_D. \tag{28}$$

The first inequality of (27) as per (15) means similarity of the characteristic times on all the spatial scales. It follows from the second inequality that the atoms displacements on the atomic scales must be small in comparison with the interatomic distances. It follows from the last inequality of (27) that there is an equality  $v_2 > v_1$ . I.e., the macroscopic deformation should be realized in the fast mechanisms, which are represented by twin formation. This peculiarity is inherent in the martensitic transformations. A physical meaning of the condition (27) is explained by reviewing Figure 2. It is clear therefrom that with the same value of the parameter  $d$  the magnitude  $\varphi_D$  decreases with increase in the parameter  $c$ , and vice versa. The parameter  $c$  characterizes increase in the system's elastic energy in formation of the new phase. Shear moduli of the solid are always smaller than a bulk modulus. So, increase in the elastic energy in shear strain is always less than in the change of the system volume. It is no surprise that in the martensitic transformations the volume changes are small, and deformation is determined by shear components.

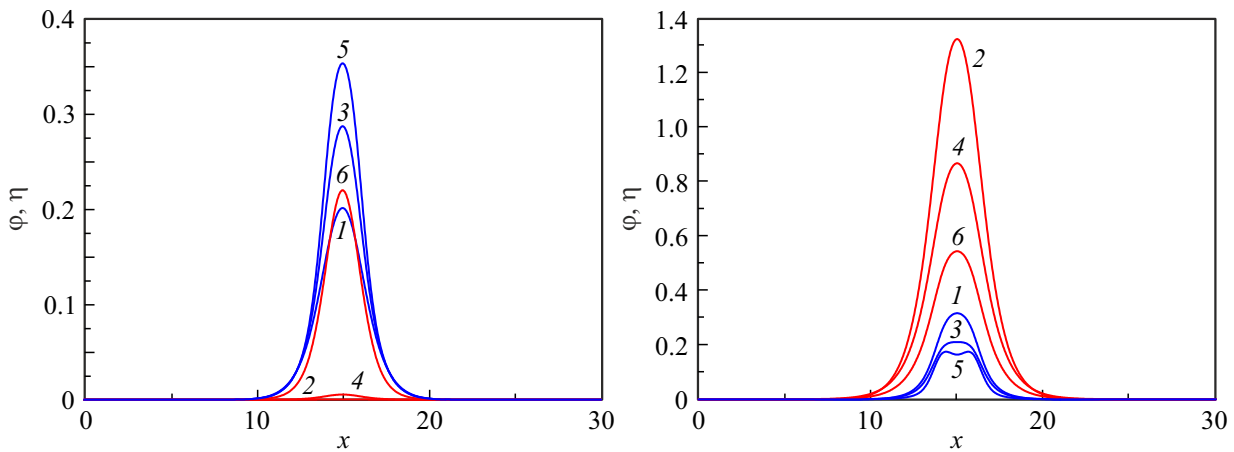


**Figure 4.** Spatial distribution of the order parameters  $\varphi$  — the blue curves (1, 3, 5),  $\eta$  — the red curves (2, 4, 6) in the static autosoliton in various points of time  $t$ . On the left panel,  $t = 5$  (1, 2), 20 (3, 4), 23 (5, 6). On the right panel,  $t = 26$  (1, 2), 35 (3, 4), 70 (5, 6).

The spatio-temporal OP distributions in nucleation and development of the static AS are shown on Figure 4 at

$$d = 10, \quad \tau = 0.9, \quad l = 0.05. \quad (29)$$

The rest parameters are the same as in (26). With the selected values of the parameters,  $\eta_D \approx 0.11$ ,  $\varphi_D \approx 0.35$ . It is clear from Figure 4 that there are three stages. At the first stage, OP  $\varphi$  increases to the value  $\varphi_{\max} \approx 0.29$  for the time  $t \approx 20$ , OP  $\eta$  is close to zero. At the second stage, OP  $\eta$  quickly increases, and to the point of time  $t \approx 26$  it is of the maximum value  $\eta_{\max} \approx 1.3$ . At the third stage, both the OPs decrease to the stationary values in the static AS.

Formation of the static AS exhibits as bands of the localized shear macroscopic strain and is accompanied by reduction of the system's elastic energy. At the same time, as per (8) the homogeneous system forms a system of regularly-arranged stable bands of localized deformation. With further change of the temperature, new bands can appear only between the previously formed bands. This situation qualitatively agrees with a situation experimentally observed in the martensitic transformations.

As clear from Figure 2, with increase in the parameter  $c$ , the stationary value of OP  $\eta_D$  reduces to  $\eta_D \approx 0.08$ . Then, with the same value of the parameter  $d$ , an oscillating AS with a periodically changing amplitude is excited. We remind that the magnitude  $c \propto \vartheta_n$ , and  $\vartheta_n$  is determined by the properties of the crystal lattices of the austenite and martensite phases. The martensitic transformation may be observed in systems, whose transition of the crystal lattice of the austenite phase into the crystal lattice of the martensite phase occurs mainly via shifts of atoms in mutually perpendicular directions along the two axes. Compression/expansion along the third axis should be slight. Thus, for example, in the TiNi alloys with TMT observed the austenite phase has the B2 structure with the lattice cell parameter  $a_A \approx 0.30$  nm, the martensite phase B19' has a monoclinically-distorted orthorhombic cell with the

parameters  $a_M \approx 0.29$  nm,  $b_M \approx 0.41$  nm,  $c_M \approx 0.46$  nm. The volume changes do not exceed several tenth percent [5].

In the reconstructive martensitic transformations in the steels  $\text{Fe}_\gamma(\text{C}) \rightarrow \text{Fe}_\alpha(\text{C})$  (C — carbon concentration), the martensite phase has a body-centered tetragonal lattice. As known, the FCC lattice can be switched into the BCC lattice via 20%-compression along one of the axes  $\langle 001 \rangle$  synchronous extensions by  $\approx 13\%$  along a pair of the orthogonal axes  $\langle 100 \rangle$ ,  $\langle 100 \rangle$  or  $\langle 110 \rangle$ ,  $\langle \bar{1}10 \rangle$  of the FCC lattice. On the atomic scales, such reconstruction is realized by means of change of the interatomic interactions. In case of carbon atoms available, the phase with the BCC crystal lattice is unstable. The phase with the BCT crystal lattice is stable. The volume changes in the martensitic transformation are small as well. This result is achieved by high rates of quenching to the temperatures below the threshold values. Therefore, it prevents decomposition of supersaturated solid solution of carbon in the  $\alpha$ -phase. The high rates of quenching and the low temperatures determine the athermic mechanism of the martensitic transformations.

The framework of the proposed model makes it possible to explain availability of the pre-transition states in TMT and absence thereof in RMT. In TMT, the parent phase is metastable. The transition into the stable phase is conditioned by (22). I.e., the systems shall have initial perturbation of OP  $\varphi$  of a finite amplitude. OP  $\varphi$  characterizes distribution of the dynamic displacements of atoms when changing the interatomic interactions. The change of the interatomic interactions with change of the temperature (volume) is accompanied by the change of the elastic constants and DSO formation. With change of the temperature, the amplitude  $\varphi$  is of a threshold value, and there is TMT against the background of the excited DSO. The DSO excitation explains the fact that the first-order phase transitions occur in the low temperatures, too. For example, in the proustite crystal ( $\text{Ag}_3\text{AsS}_3$ ) in the equilibrium conditions, the first-order phase transition takes place at the temperature  $T_{c0} = 28\text{--}30$  K [34]. In the non-

equilibrium conditions (with increase in the velocity of heating/cooling), the perturbation of the finite amplitude will be achieved within a smaller period of time. It is equivalent to the fact that the temperature of the non-equilibrium phase transition will be above  $\theta_c$  in cooling and below  $\theta_c$  in heating. It is exactly this pattern that is observed experimentally [34].

In RMT, the dynamic displacements of the atoms result in formation of the unstable  $\alpha$ -phase with the BCC lattice. As per (23), the time of its formation is in reverse proportion to the velocity of cooling. No perturbation of the finite amplitude is required for the transition from the unstable phase into the martensite phase with the BCT lattice. The energy range between the PESes increases with decrease in the system volume (the number of atoms), and the probability of the nonadiabatic transitions decreases. As a consequence, RMT in such systems may be difficult, or may not occur at all.

## 7. Conclusion

The proposed model of the phase transformations in the solids has taken into account processes, which occur in the open system on the various spatio-temporal scales. On the atomic scales, the dynamics of atoms is nonadiabatic, there are the two mechanisms of the atoms displacements: the thermally activated one and the athermal one. The dynamics of the system on the large scales is determined by the collective (correlated) displacements of atoms and described by the two order parameters — the amplitudes of the unstable modes, which are excited on the thresholds of system stability. The thresholds of stability are determined by thermodynamic characteristics and equations of state for the two phases. The instability development on all the spatio-temporal scales is accompanied by reduction of the system's potential energy.

The kinetics of the phase transformation is described by the two coupled non-linear equation of a parabolic type for the order parameters. The governing parameters of the equations are the macroscopic characteristics of the system: the temperature (the volume of the metastable phase) and the difference of the volumes of the two phases. Based on analysis of the solutions of the equations, conditions have been found, at which various kinetics patterns of the phase transformations are realized.

The diffusion phase transformations occur in the systems, in which the difference of the volumes of the two phases is comparatively great. The nucleation and growth of the new phase are described by the solutions in the form of the wave of switching from the metastable phase into the stable one. The nucleation of the new phase is caused by the athermal displacements of the atoms. There is the incubation period of nucleation and growth of the embryo. Depending on the temperature change rate, the transition from one phase into another can be in the mode of overcooling/overheating or in the mode of „explosive“ transformation.

The martensitic transformations occur in the systems, whose transformation of the crystal lattices in the phase transition is accompanied by the small change of the volume and the large shear strains. The solutions of the equations, which describe the forming martensite phase, are static autosolitons. The thermoelastic martensitic transformations develop against the background of the displacements, which are determined by the change of the interatomic interactions in the transition from one crystal lattice into another. The formed short-range order, which is non-typical for the metastable phase, acts as embryos of the martensite phase. In the reconstructive martensitic transformations, which occur in the non-equilibrium conditions, the formed short-range order is typical for the unstable phase. Therefore, no embryo is required for formation of the martensite phase.

Thus, the model of the phase transformations in the solids (which is comparatively simple in terms of mathematics) leads to results, which qualitatively agree with the available experimental data. It means that the model takes into account the main physical processes that occur in the open system of nuclei and electrons in the phase transformation.

## Appendix

The equations (13), (14) have been numerically solved using the finite-difference method with a completely implicit scheme in the interval  $0 \leq x \leq X$ . At  $t = 0$ , the system is in the state  $\eta_0, \varphi_0$ . The initial perturbation for the variable  $\varphi$  was specified as

$$\Delta\varphi = \Delta\varphi_0 \exp[-\sigma_\varphi(x - x_0)^2].$$

Here,  $\delta\varphi_0, \sigma_\varphi, x_0$  — the amplitude, dispersion and the coordinate of the initial perturbation, respectively. The initial perturbation for the variable  $\eta$  is accepted to be a stochastic one with the amplitude  $0 \leq \Delta\eta(x) \leq 10^{-3}$ . Periodic boundary conditions were set.

## Acknowledgments

The author would like to thank S.P. Belyaev, A.E. Volkov, L.B. Zuev, A.I. Lotkov, N.N. Resnina, H. Zapolsky for their interest in the study, useful advice and comments.

## Funding

The paper was prepared under the state assignment of the Institute of Strength Physics and Materials Science of the Siberian Branch of the Russian Academy of Science, subject No. FWRW-2021-0011.

## Conflict of interest

The author declares that he has no conflict of interest.

## References

- [1] Ya.B. Zeldovich. ZhETF **12**, 525 (1942). (in Russian).
- [2] J. Christian. The Theory of Transformations in Metals and Alloys. Pergamon Press (1965). V. 1.
- [3] Nucleation theory and application/ Ed. J.W.P. Schmelzer. Wiley-VCH (2006). 453 p.
- [4] E.M. Lifshitz, L.P. Pitaevskii. Physical Kinetics. Pergamon, London, UK (1981).
- [5] V.G. Pushin, V.V. Kondratiev, V.N. Khachin. Predperekhodnye yavleniya i martensitnye prevrascheniya. UrO RAN, Yekaterinburg (1998), 368 s. (in Russian).
- [5] A.I. Potekaev, A.A. Klopotov, V.V. Kulagina, Yu.V. Solovieva, S.G. Anikeev. Struktura i svoistva splavov na osnove NiTi v predperekhodnykh slaboustoichivyykh sostoyaniakh / Pod red. A.I. Potekaeva. Izd-vo NTL, Tomsk (2021), 360 s. (in Russian).
- [6] V. Dmitriev. Discontinuous Phase Transitions in Condensed Matter. World Scientific (2023). 439 p.
- [7] Wen-Zheng Zhang. Crystals **10**, *11*, 1042 (2020). doi.org/10.3390/cryst10111042
- [8] G.A. Malygin. UFN **171**, 187 (2001). [G.A. Malygin. Phys.-Usp. **44**, 2, 173 (2001).] (in Russian).
- [9] M.P. Kashchenko, V.G. Chashchina. Phys.-Usp. **54**, 4, 331 (2011).
- [10] G.A. Malygin. Phys. Solid State **64**, 5, 563 (2022).
- [11] A.L. Roitburd. Sov. Phys. Usp. **17**, 326 (1974).
- [12] G.E. Abrosimova, D.V. Matveev, A.S. Aronin. Phys.-Usp. **65**, 3, 227 (2022).
- [13] V. Levitas. Int. J. Plast. **140**, 102914 (2021). <https://doi.org/10.1016/j.ijplas.2020.102914>.
- [14] S.A. Kukushkin, A.V. Osipov. Prog. Surf. Sci. **151**, 11 (1996). DOI: 10.1016/0079-6816(96)82931-5.
- [15] S.A. Kukushkin, A.V. Osipov. Phys.-Usp. **41**, 10, 983 (1998).
- [16] S.A. Kukushkin, A.V. Osipov. Phys. Solid State **56**, 4, 792 (2014).
- [17] A.L. Murtazaev, M.K. Ramazanov. FTT **65**, 9, 1455 (2023). (in Russian). DOI: <http://dx.doi.org/10.21883/FTT.2023.09.56240.114>
- [18] T.R. Kirkpatrick, D. Thirumalai. Rev. Mod. Phys. **87**, 183 (2015). DOI: 10.1103/RevModPhys.87.183
- [19] L. Landau. Phys. Z. Sowjetunion. **2**, 46 (1932).
- [20] C. Zener. Proc. R. Soc. London A **137**, 696 (1932).
- [21] E.C.G. Stückelberg. Helv. Phys. Acta **5**, 369 (1932).
- [22] E. Majorana. Nuovo Cimento **9**, 43 (1932).
- [23] C. Zhu, H. Nakamura. J. Chem. Phys. **101**, 10630 (1994).
- [24] C. Zhu, H. Nakamura. J. Chem. Phys. **102**, 7448 (1995).
- [25] V.E. Egorushkin, N.V. Mel'nikova. JETP **76**, 1, 103 (1993).
- [26] Yu.A. Khon. Phys. Solid State **65**, 8, 1211 (2023). DOI: 10.21883/PSS.2023.08.56564.100.
- [27] L.I. Sedov. Mekhanika sploshnoi sredy. Nauka, M., (1976), T. 1. 536 s. (in Russian).
- [28] J.C. Tully. J. Chem. Phys. **137**, 22A301 (2012).
- [29] B.F.E. Curchod, U. Rothlisberger, I. Tavernelli. Chem. Phys. Chem. **14**, 1314 (2013).
- [30] P.C. Hohenberg, A.P. Krekhov. Phys. Rep. **572**, 1 (2015).
- [31] Yu.A. Khon, L.B. Zuev. Phys. Mesomech. **25**, 111 (2022) DOI: 10.1134/S1029959922020023.
- [32] V.A. Shklovskii, V.M. Kuzmenko. Phys.-Usp. **32**, 2, 163 (1989).
- [33] B.S. Kerner, V.V. Osipov. Phys.-Usp. **32**, 2, 101 (1989).
- [34] I.M. Shmytko, I.M. Afonnikova, N.S. Dorokhova. FTT **40**, 2217 (1998). (in Russian).

*Translated by M. Shevelev*